



Peptidomimetic modification improves cell permeation of bivalent farnesyltransferase inhibitors



Shinnosuke Machida^a, Mai Tsubamoto^a, Nobuo Kato^a, Kazuo Harada^b, Junko Ohkanda^{a,*}

^aThe Institute of Scientific and Industrial Research, Osaka University, 8-1 Mihogaoka, Ibaraki, Osaka 567-0047, Japan

^bDepartment of Life Sciences, Tokyo Gakugei University, Koganei, Tokyo 184-8501, Japan

ARTICLE INFO

Article history:

Available online 11 October 2012

Keywords:

Bivalent inhibitors
Farnesyltransferase
K-Ras4B
Protein–protein interaction
Whole cell activity

ABSTRACT

Bivalent enzyme inhibitors, in which a surface binding module is linked to an active site binding module through a spacer, are a robust approach for site-selectively delivering a minimally-sized agent to a protein surface to regulate its functions, such as protein–protein interactions (PPIs). Previous research revealed that these agents effectively disrupt the interaction between farnesyltransferase (FTase) and the C-terminal region of K-Ras4B protein. However, the whole cell activity of these peptide-based agents is limited due to their low membrane permeability. In this study, we tested a peptidomimetic modification of these bivalent agents using a previously developed inhibitor, FTI-249, and evaluated their cell permeability and biological activity in cells. Confocal cell imaging using fluorescently-labeled agents showed that the peptidomimetic **3-BODIPY** penetrated cells, while the peptide-based **1-BODIPY** did not. Cell-based evaluation demonstrated that peptidomimetic **3** at a concentration of 100 μ M inhibited HDJ-2 processing in cells, indicating that this peptidomimetic modification improves cell permeability, thus leading to enhanced whole cell activity of the bivalent compounds.

© 2012 Elsevier Ltd. All rights reserved.

1. Introduction

Low-molecular-weight compounds that disrupt protein–protein interactions (PPIs) hold tremendous potential for medicinal purposes and for probing intracellular PPI networks.^{1,2} However, the development of drug-like molecules that control PPIs remains difficult since the interacting interfaces often lack structurally defined cavities. Antibodies are the ultimate example of multivalent agents capable of binding to large protein surfaces in an aqueous environment, but their therapeutic application is limited, in part due to their inability to permeate cells and their poor oral bioavailability.³ New strategies for reducing molecular size while retaining binding selectivity are required for developing PPI-directed inhibitors. We recently reported a new approach for designing PPI-directed agents based on module assembly,⁴ in which small module compounds are designed to bind in a complementary fashion to several targeted areas of the protein surface. These compounds are assembled by various means to generate a multivalent agent that is more capable of surface recognition than each module compound individually. One approach used is the anchoring strategy (Fig. 1). We predicted that bivalent compounds derived by covalent linking of a surface binding module (red in Fig. 1) to an anchoring module via a spacer of appropriate length would allow selective binding and reduce the

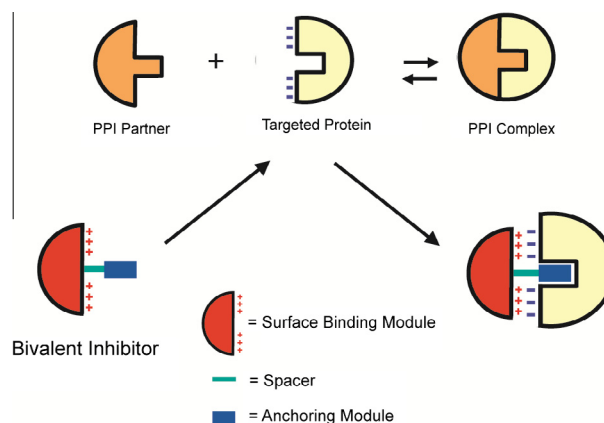
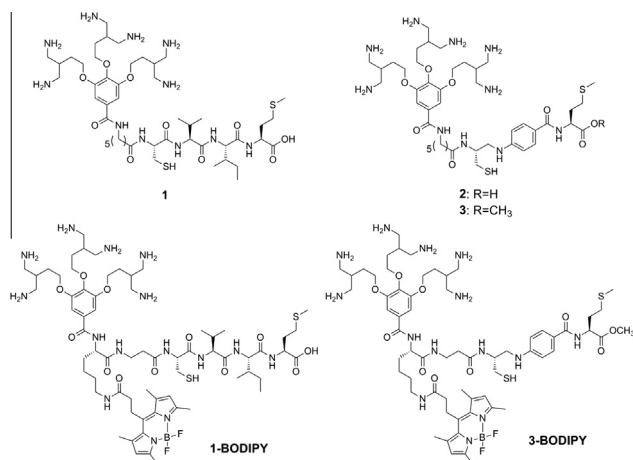


Figure 1. A schematic representation of the module assembly strategy for anchor-based PPI inhibitors.

molecular size of the PPI-directed inhibitor. This hypothesis was validated in our previous study^{4a} based on in vitro evaluation of bivalent compound **1** (Scheme 1). Compound **1** was designed to bind to the active site and the acidic surface of protein farnesyltransferase (FTase), which interacts through PPIs with K-Ras4B protein.⁵ Compound **1** was found to inhibit farnesylation of a peptide derived from the K-Ras4B C-terminal two orders of magnitude more efficiently than the two modules individually,^{4a} but further

* Corresponding author.

E-mail address: johkanda@sanken.osaka-u.ac.jp (J. Ohkanda).



Scheme 1. Chemical structures of bivalent compounds used in this study.

biological evaluation was hampered by the inactivity of **1** in whole cells.

Human K-Ras4B is the most mutated Ras isoform in cancers,⁶ therefore inhibitors for the posttranslational farnesylation process of K-Ras4B have been intensely investigated.⁷ However, full suppression of K-Ras prenylation by conventional FTase inhibitors is difficult due to the transient PPIs with FTase. These PPIs are driven by electrostatic interaction between the polylysine domain and the acidic surface of FTase.⁵ Thus, cell permeable, PPI-directed, synthetic FTase inhibitors may provide a new platform for antitumor agents for K-Ras mutated human carcinomas. This prompted us to study a simple structural modification of **1** using a previously

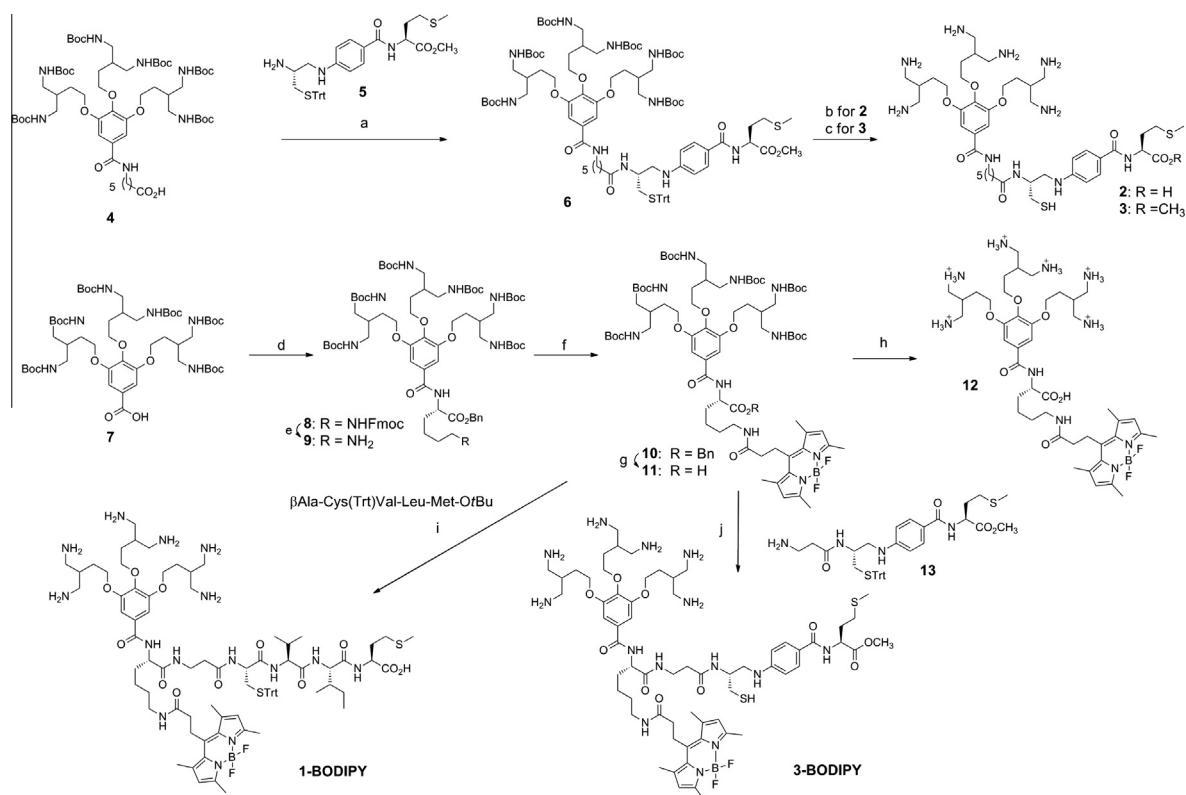
reported peptidomimetic compound⁸ and test whether this modification could address these problems. Herein we report the synthesis of peptidomimetic-containing bivalent compounds, the results of FTase assays, the evaluation of membrane penetration using confocal fluorescence microscopy, and the results of cell-based assays for evaluating FTase inhibition.

2. Results and discussion

2.1. Design and synthesis

Previously, we designed compound **1** using the tetrapeptide anchor module CVIM, which is the C-terminal four amino acid sequence of K-Ras4B. This peptidic anchor module was linked to a galate module containing six amino groups for electrostatic interaction with the acidic surface of FTase. Peptidomimetic approaches for developing FTase inhibitors have been intensively studied over the past decades and have made a major contribution to cancer therapy.⁹ An earlier example, developed by Sebti and Hamilton,⁸ is FTI-249 (IC₅₀ for FTase = 300 nM), which was designed to mimic an extended conformation of the CVIM tetrapeptide. The hydrophobic VI dipeptide moiety was replaced by a 4-amino benzoic acid scaffold. Its methyl ester pro-drug form **5** was found to be active in whole cells at 200 μM, although CVIM itself was inactive.⁸ Thus, we decided to replace the CVIM module in **1** with FTI-249 and its corresponding methyl ester form to give **2** and **3**, respectively (Scheme 1). To examine whether these replacements improve membrane penetration of the compounds, we also designed fluorescently-labeled derivatives using the BODIPY chromophore for confocal cell imaging to give **1-BODIPY** and **3-BODIPY**.

The synthetic approach to compounds **2–3** and **1**, **3-BODIPY** is shown in Scheme 2. Compounds **2** and **3** were synthesized by



Scheme 2. Reagents and conditions: (a) **5**, HOBT, PyBOP, 73%; (b) KOH in MeOH, then 30% TFA and 5% TES in dichloromethane, 70%; (c) 50% TFA and 5% TES in dichloromethane, 27%; (d) H-Lys(Fmoc)-OBn, HOBT, PyBOP, 67%; (e) diethylamine; (f) BODIPY, HOBT, PyBOP, 99%; (g) Pd(OH)₂, 62%; (h) 30% TFA in dichloromethane, 68%; (i) βAla-Cys(Trt)-Val-Met-OfBu, HOBT, PyBOP, 65%, and then 50% TFA and 5% TES in dichloromethane, 20%; (j) **13**, HOBT, PyBOP, 65%, and then 50% TFA and 5% TES in dichloromethane, 20%.

coupling reaction of Boc-protected gallate **4**^{4a} with peptidomimetic **5**, followed by deprotection. To synthesize the BODIPY-containing compounds, the linear alkyl spacer used in **1** and **3** was replaced by a lysyl- β -alanine dipeptide of similar length. Coupling of **7** with ω -Fmoc-L-lysine benzyl ester followed by deprotection gave **9**, which was then coupled with BODIPY carboxylic acid using HOBt/PyBOP to afford compound **10**. After removal of the benzyl group by hydrogenation, the resulting free acid **11** was coupled either with protected tetrapeptide β Ala-Cys(Trt)-Val-Leu-Met-OtBu or compound **13** to give protected precursors; these precursors were then deprotected by acid treatment to afford **1-BODIPY** and **3-BODIPY**, respectively.

2.2. In vitro FTase inhibition assay

First, we evaluated the compounds using an in vitro FTase inhibition assay, in which farnesylation of the dansylated K-Ras4B model peptide (KKKKKSK(Dans)TKCVIM) was monitored. The procedure was similar to that previously reported, except that in this study all the kinetic measurements were performed on a fluorescence microplate reader to shorten the experiment. Briefly, in a well of a 96-well black plate, 10 μ L of each stock solution of farnesylpyrophosphate (FPP, 100 μ M), K-Ras4B peptide (20 μ M), recombinant FTase (2 μ M), and test compound were spotted so that the spots did not touch. Then, 160 μ L of buffer solution was then added, resulting in mixing of the spotted solutions, thus initiating the enzyme reaction. The time-course change of the fluorescence intensity was monitored at 520 nm (ex: 340 nm) for 5 min. Figure 2 shows three replicate sets of data in the absence (purple) or the presence (red) of inhibitor. The data demonstrate reasonable reproducibility, with a standard deviation of <3.5%. This procedure significantly shortened the time required to evaluate each compound, from 6 to 7 h to less than 60 min.

The percentage of inhibition was calculated by comparison with the standard slope, obtained from the reaction in the absence of inhibitors. The IC_{50} values were converted to the inhibition constant (K_i) using the Cheng-Prusoff equation.¹⁰ The results are

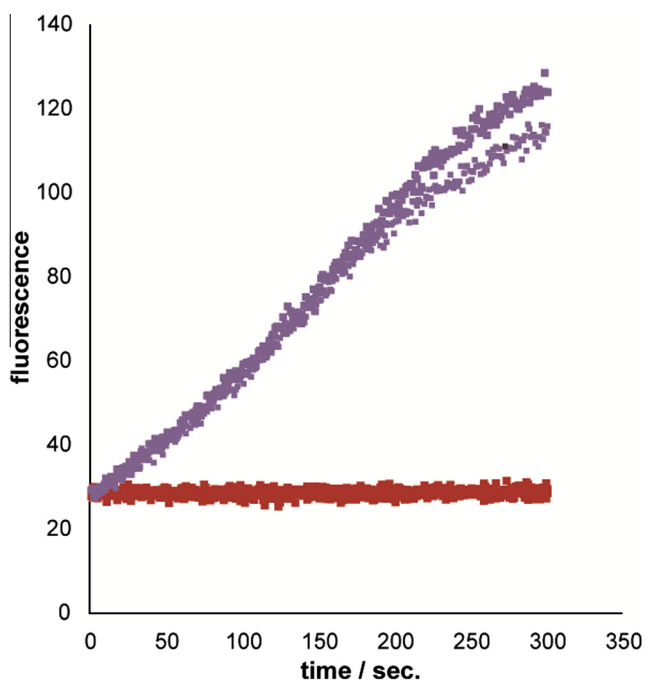


Figure 2. The time course fluorescence change at 520 nm (ex: 340 nm) in the absence (purple) or in the presence (red) of inhibitor. Three replicate data sets are presented.

Table 1
Inhibition of farnesylation of the K-Ras4B model peptide^a

compound	K_i (μ M) ^b
CVIM	1.10 \pm 0.29 ^c
FTI-249	0.785 \pm 0.008
1	0.015 \pm 0.008 (0.005 \pm 0.001) ^c
2	0.837 \pm 0.018

^a Fluorescent in vitro assay were performed in a 96-well black plate using KKKKKKSK(Dans)TKCVIM (1 μ M), FPP (5 μ M), compounds (0–500 μ M), and FTase (50 nM) in 50 mM Tris HCl (pH 7.5) at 30 $^{\circ}$ C. The reaction was monitored at 520 nm (ex. 340 nm) for 5 min by a plate reader. The standard deviation is given for $n = 3$.

^b K_i values were obtained by conversion of IC_{50} values using the Cheng-Prusoff equation (ref. 10): $K_i = IC_{50}/(1 + ([S]/K_m))$, where $K_m = 0.033 \pm 0.008$ μ M determined for the K-Ras4B peptide previously (Ref. 4a).

^c Ref. 4a.

summarized in Table 1. Peptidomimetic FTI-249 inhibited farnesylation of the model peptide, with a K_i value of 0.785 μ M, confirming that this peptidomimetic possesses a similar potency to that of CVIM tetrapeptide, as previously reported.⁸ High inhibition by bivalent compound **1** of farnesylation of the K-Ras4B peptide was confirmed by the microplate reader assay, indicating that the anchored gallate module effectively disrupted the interaction between FTase and the peptide. Somewhat surprisingly, bivalent compound **2**, containing the FTI-249 moiety, remained a moderate inhibitor, with a K_i value similar to that of FTI-249. This suggests that **2** failed to deliver the gallate to the acidic surface of FTase, or had lost the affinity of the FTI-249 portion for the FTase active site and this loss in affinity was compensated for by the gallate binding to the surface of FTase. A possible explanation for the latter case is that the covalent linking of the gallate module to FTI-249 may alter the conformation of the peptidomimetic in the FTase active site and thus interfere with its zinc coordination.

2.3. Cell permeating properties of BODIPY-attached compounds

Next, we tested the cell permeation of the fluorescently-labeled compounds using lung adenocarcinoma epithelial A549 cells. Cells were treated with 25 μ M of **12**, **1-BODIPY**, or **3-BODIPY**, and confocal images were observed (Fig. 3). Gallate derivative **12** was found to enter cells (Fig. 3A), demonstrating that the highly positively-charged module does not interfere with membrane penetration. In contrast, **1-BODIPY** accumulated on the plasma membranes, and no penetration was detected (Fig. 3B and Fig. S1). These results suggest that the low cell permeability of **1-BODIPY** is likely due to the polar CVIM anchor. This is consistent with the fact that the CVIM tetrapeptide is inactive in cells.⁸ In contrast, **3-BODIPY** enters cells and becomes localized in the cytosol rather than in the nucleus (Fig. 3C and Fig. S2), indicating that the peptidomimetic modification of CVIM improves membrane penetration.

2.4. Inhibition of prenylation processing in cells

Finally, inhibition by peptidomimetic **3** was evaluated in cells. Whole cell inhibition of farnesylation and geranylgeranylation was determined by a procedure similar to that previously reported in the literature,¹¹ based on the level of inhibition of HDJ-2 and Rap1A processing, respectively. Oncogenic H-Ras-transformed human bladder carcinoma T24 cells or A549 cells were treated with various concentrations of inhibitors twice on day 1 and day 3 and then incubated for 4 days. The cell lysates were separated on 7.5% sodium dodecyl sulfate polyacrylamide gels by electrophoresis. The separated proteins were transferred to a polyvinylidene difluoride membrane and immunoblotted using anti-HDJ-2 (ab3089) or anti-Rap1A (SC-65) antibody. Antibody reactions were visualized using HRP-conjugated anti-rabbit IgG and an enhanced

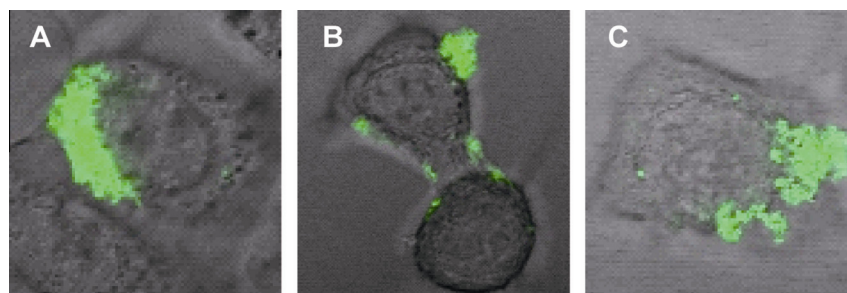


Figure 3. A549 cells were treated with compounds (25 μM) and incubated at 37 $^{\circ}\text{C}$ for 3 h. The samples were analyzed under a confocal microscope. Enlarged images for comparison, A: **12**, B: **1-BODIPY**, and C: **3-BODIPY** (also see Fig. S1 and S2).

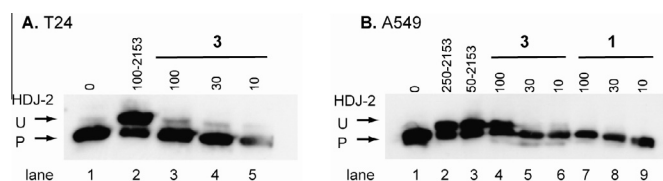


Figure 4. Effect of compounds on processing of HDJ-2 in (A) T24 and in (B) A549 cells. Western blot analysis demonstrates the inhibition of farnesylated HDJ-2 as seen by the band shift from processed (P) to unprocessed (U) protein. (A) lane 1: vehicle control; lane 2: 100 μM FTI-2153; lane 3–5: 100, 30, 10 μM **3**. (B) lane 1: vehicle control; lane 2–3: 250, 50 μM FTI-2153; lane 4 to 6: 100, 30, 10 μM **3**; lane 7–9: 100, 30, 10 μM **1**.

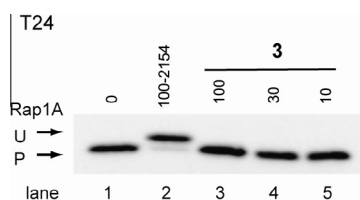


Figure 5. Effect of compounds on processing of Rap1A in T24 cells. The inhibition of geranylgeranylated Rap1A was seen by the band shift from processed (P) to unprocessed (U) protein. Lane 1: vehicle control; lane 2: 100 μM GGTI-2154; lane 3–5: 100, 30, 10 μM **3**.

chemiluminescence detection system. As a reference, FTI-2153¹² and GGTI-2154¹³ were used for HDJ-2 and Rap1A processing inhibition, respectively. The results of the Western blot are shown in Figure 4 and Figure 5. Compound **3** inhibited HDJ-2 processing in T24 cells (Fig. 4A, lane 3–5) and in A549 cells (Fig. 4B, lane 4–6) at concentrations between 10 and 100 μM . In contrast, CVIM-based **1** was found to be inactive under the same conditions (Fig. 4B, lane 7–9). The difference in whole cell activity of **1** and **3** can be accounted for by the results of confocal microscopy using **1-BODIPY** and **3-BODIPY**, described above. Importantly, compound **3** did not inhibit Rap1A processing (Fig. 5), thus demonstrating that **3** does not interfere with native GGTase-I processing in cells. These results verified that peptidomimetic modification of the anchor module improves membrane penetration of the compounds, resulting in whole cell inhibition of FTase.

3. Conclusions

We conducted peptidomimetic modification of a previously developed bivalent inhibitor of FTase, and investigated its membrane penetration and whole cell inhibition activity against FTase. Confocal imaging of BODIPY-labeled compounds showed that replacement of the CVIM anchor by a peptidomimetic FTI-249 improved membrane penetration, although such modification

somewhat reduced in vitro potency against FTase. The results of cell-based assays showed that the peptidomimetic **3** inhibited FTase processing, while the peptidic **1** was inactive. This indicates that peptidomimetic modification is a promising approach for the development of bivalent inhibitors targeting intracellular PPIs. Reduced in vitro activity observed for **2** suggests that further structural modifications of the surface module and the peptidomimetic-based anchor module are necessary to improve the activity. The moderate membrane penetration ability of **3-BODIPY** observed in the confocal imaging needs to be improved for better cell activity. Work based on guanidino groups to address this issue is currently in progress in our laboratory.

4. Experimental section

4.1. Chemistry

4.1.1. General

Reagents and solvents were obtained from commercial sources without further purification unless otherwise noted. ^1H and ^{13}C NMR spectra were recorded on a JEOL JNM-LA 400 spectrometer. Chemical shifts were reported in δ (ppm) relative to tetramethylsilane. All coupling constants were described in Hz. Elemental analyses were performed using Perkin Elmer-2400CHN in Material Analysis Center of ISIR. Flash column chromatography was performed on silica gel (40–63 μm) under a pressure of about 4 psi. HPLC measurements were performed using a JASCO PU-2086 and a JASCO UV-2075 detector with a GL Science Inertsil 150 \times 4.6 mm, 5 μm C-18 column, eluted with gradient 10–90% of CH_3CN in 0.1% TFA in H_2O in 30 min. High-resolution mass spectra (HRMS) and low-resolution mass spectra (LRMS) were taken by Professors T. Maki and N. Yamaguchi from Nagasaki University Instrument Center. Compounds **1**, **4** and **7**, ^{4a} and **5** and FTI-249 (Cys-4ABA-Met-OCH₃)¹⁴ were prepared by the previously reported methods.

4.1.2. Synthesis of peptidomimetic compounds

4.1.2.1. 4,4-Difluoro-8-(butyl-4-carboxyl)-1,3,5,7-tetramethyl-4-bora-3a,4a-diaza-s-indacene (BODIPY free acid). A solution of succinic anhydride (1.0 g, 10 mmol), benzyl alcohol (1.14 g, 11 mmol), and DMAP (54 mg, 0.44 mmol) in THF (5 mL) was refluxed for 18 h. The mixture was basified with sat. NaHCO_3 , and washed with AcOEt. The aqueous layer was then acidified, and the precipitated solid was extracted with AcOEt. The solid was recrystallized to afford succinic acid monobenzyl ester as colorless needles, 1.85 g, 88%. ^1H NMR (400 MHz, CDCl_3) δ : 2.65–2.73 (m, 4H, CH_2CH_2), 5.15 (s, 2H, PhCH_2), and 7.31–7.38 ppm (s, 5H, aromatic).

The carboxylic acid (1.02 g, 4.9 mmol) was reacted with oxalyl chloride (1.1 mL, 13 mmol) in the presence of catalytic amount of DMF in dichloromethane (40 mL) at rt for 1.5 h, and concentrated. To a solution of 2,4-dimethylpyrrole (713 mg, 7.3 mmol) in

dichloromethane (20 mL) was added the acid chloride in dichloromethane (10 mL), and the mixture was refluxed for 1 h. After cooling to rt, to the solution was added triethylamine (3.5 mL, 25 mmol) in toluene (32 mL) and boron trifluoride diethyl ether (3.1 mL, 25 mmol), then stirred at 50 °C for 1 h. The product was extracted with dichloromethane, and purified by SiO₂ column chromatography to give 4,4-difluoro-8-(butyl-4-carboxybenzyl)-1,3,5,7-tetramethyl-4-bora-3a,4a-diaza-s-indacene as a green amorphous solid, 904 mg, 47%. ¹H NMR (400 MHz, CDCl₃) δ. 2.41 (s, 6H, CH₃-dipyrrin), 2.51 (s, 6H, CH₃-dipyrrin), 2.62–2.67 (m, 2H, CH₂CO₂Bn), 3.29–3.34 (m, 2H, CCH₂), 5.17 (s, 2H, CH₂Ph), 6.05 (s, 2H, CH-dipyrrin), and 7.32–7.39 ppm (m, 5H, aromatic from benzyl): LRMS-ESI (*m/z*): [M+Na]⁺ Calcd for C₂₃H₂₅BF₂N₂NaO₂, 433. Found 433.

The benzyl ester (112 mg, 0.27 mmol) was removed by hydrogenation with Pd(OH)₂ (10 mg) in MeOH to give the desired product as a red oil (96 mg, 99%). ¹H NMR (400 MHz, CDCl₃) δ. 2.45 (s, 6H, CH₃-dipyrrin), 2.52 (s, 6H, CH₃-dipyrrin), 2.64–2.69 (m, 2H, CH₂CO₂Bn), 3.31–3.35 (m, 2H, CCH₂), and 6.08 ppm (s, 2H, CH-dipyrrin).

4.1.2.2. N-(5-[3,4,5-Tris[3-(1,3-(N,N'-t-butoxycarbonyl)diaminopropyl]-1-propanoxy]benzoylamino]hexanylcarbonyl)-4-[N-[2(R)-amino-3-(triphenyl-methyl)thio]propyl]-aminobenzoyl]-methionine methyl ester (6). Compound 4 (113 mg, 0.096 mmol) was coupled with peptidomimetic 5 (0.12 mmol) using PyBOP (81 mg, 0.16 mmol), HOBt (31 mg, 0.20 mmol), and DIEA (0.20 mmol) in DMF (3 mL). The crude product was purified by silica gel column chromatography to give the desired product as colorless solid, 125 mg, 73%. ¹H NMR (400 MHz, CDCl₃) δ 1.43 (s, 54H, CH₂CH₂CH₂CONH, Boc × 6), 1.58–1.84 (m, 13H, 3,4,5-CH₂CH, CH₂CH₂CO, NHCH₂CH₂), 2.01–2.15 (m, 6H, SCH₃, γ-CH₂ Met, and β-CH_a Met), 2.19–2.28 (m, β-CH_b Met), 2.44 (dd, 1H *J* = 5.3 and 12.5 Hz, β-CH_a Cys), 2.51–2.59 (m, 3H, -CH_b Cys, CH₂CONH), 3.05–3.20 (m, 14H, 3,4,5-CH₂NHBoc, and CH₂NHPh), 3.32–3.39 (m, 2H, CONHCH₂), 3.75 (s, 3H, CO₂CH₃), 4.04–4.09 (3,4,5-OCH₂, α-CH Cys, and NHPh), 4.83–4.88 (m, 1H, α-CH Cys), 5.58–5.65 (m, 7H, NHBoc × 6, and CH₂NHCO), 6.46 (d, 2H, *J* = 8.6 Hz, aromatic ring from benzoyl), 6.82 (m, 1H, CONHCH₂), 6.95 (m, 1H, NH Met), 7.05 (s, 2H, aromatic from gallate), 7.20–7.41 (m, 15H, aromatic from Trt), and 7.58 ppm (d, 2H, *J* = 8.5 Hz, aromatic from benzoyl): LRMS-ESI (*m/z*): [M+H]⁺ Calcd for C₉₃H₁₃₈N₁₀NaO₂₀S₂, 1802.9. Found; 1802.8.

4.1.2.3. N-(5-[3,4,5-Tris[3-(1,3-diaminopropyl)-1-propanoxy]benzoylamino]hexanylcarbonyl)-4-[N-[2(R)-amino-3-mercapto propyl]-aminobenzoyl]-methionine TFA salt (2). Compound 6 (22 mg, 0.013 mmol) was hydrolyzed with 2 M KOH (200 μL) in MeOH (1.5 mL) under reflux condition for 1 h. The solution was acidified with 10% citric acid, and the resulting free carboxylic acid was extracted with dichloromethane, and the protecting groups were then removed by 30% trifluoroacetic acid in dichloromethane in the presence of 5% triethylsilane. The crude material was purified by preparative HPLC to give the desired product as colorless solid, 14 mg, 70%. ¹H NMR (400 MHz, DMSO-*d*₆) δ 1.28 (m, 2H, CH₂CH₂CH₂CO), 1.50 (m, 4H, CONHCH₂CH₂CH₂CH₂), 1.80–1.88 (6H, 3,4,5-CH₂CH₂, β-CH Val, and β-CH₂ Met), 2.01–2.10 (8H, 3,4,5-CHCH₂, β-CH₂ and Met, SCH₃), 2.26–2.31 (m, 2H, γ-CH₂ Met), 2.62–2.73 (m, 2H, CH₂SH), 2.60–2.78 (m, 2H, β-CH Cys), 3.00 (12H, 3,4,5-CHCH₂), 3.92–4.05 (6H, 3,4,5-OCH₂, α-CH), 4.44 (m, 1H, α-CH Met), 6.26 (br s, 1H, CH₂CONH), 6.61 (d, 2H, *J* = 8.2 Hz, aromatic) 7.21 (s, 2H, aromatic from gallate), 7.65 (d, 2H, *J* = 8.8 Hz, aromatic), 7.77 (d, 1H, *J* = 7.1 Hz, CONH), 8.03–8.15 (br s, 19H, 3,4,5-CH₂NH₃⁺ × 6, and CONH), and 8.41 ppm (1H, CONH): LRMS-FAB (*m/z*): [M+H]⁺ Calcd for C₄₃H₇₅N₁₀O₈S₂, 923.5; found; 923.4, HRMS-FAB (*m/z*): [M+H]⁺ Calcd for C₄₃H₇₅N₁₀O₈S₂, 923.5211. Found; 923.5204.

4.1.2.4. N-(5-[3,4,5-Tris[3-(1,3-diaminopropyl)-1-propanoxy]benzoylamino]hexanylcarbonyl)-4-[N-[2(R)-amino-3-mercapto propyl]-aminobenzoyl]-methionine methyl ester (3). Compound 6 (40 mg, 0.022 mmol) was treated with 50% of trifluoroacetic acid and 5% triethylsilane in dichloromethane at 30 °C. The reaction was monitored by HPLC until the starting material disappeared. The crude material was purified by preparative HPLC to give the desired product as a white solid, 10 mg, 27%. ¹H NMR (400 MHz, DMSO-*d*₆) δ 1.29 (m, 2H, CH₂CH₂CH₂CO), 1.51 (m, 4H, CONHCH₂CH₂CH₂CH₂), 1.80–1.89 (6H, 3,4,5-CH₂CH₂, β-CH Val, and β-CH₂ Met), 2.03–2.13 (8H, 3,4,5-CHCH₂, β-CH₂ Met, and SCH₃), 2.66 (1H, CH₂aSH), 2.60–2.78 (m, 2H, β-CH Cys), 3.00–3.07 (m, 12H, 3,4,5-CHCH₂), 3.62 (s, 3H, CO₂CH₃), 3.94–4.07 (6H, 3,4,5-OCH₂, α-CH), 4.51 (m, 1H, α-CH Met), 6.25 (br s, 1H, CH₂CONH), 6.63 (d, 2H, *J* = 7.1 Hz, aromatic) 7.20 (s, 2H, aromatic from gallate), 7.64 (d, 2H, *J* = 8.0 Hz, aromatic), 7.77 (d, 1H, *J* = 7.1 Hz, CONH), 8.00 (br s, 18H, 3,4,5-CH₂NH₃⁺ × 6), 8.27 (1H, CONH), and 8.38 ppm (1H, CONH), LRMS-FAB (*m/z*): [M+H]⁺ Calcd for C₄₄H₇₇N₁₀O₈S₂, 937.5; found; 937.5, LRMS-FAB (*m/z*): [M+H]⁺ Calcd for C₄₄H₇₇N₁₀NaO₈S₂, 959.5187. Found; 959.5179.

4.1.2.5. N-[3,4,5-Tris[3-(1,3-(N,N'-tert-butoxycarbonyl)diaminopropyl]-1-propanoxy]benzoyl-L-lysine benzyl ester (8). A solution of compound 7 (119 mg, 0.11 mmol), H-Lys(Fmoc)-OBn tosylate (119 mg, 0.18 mmol), HOBt (34 mg, 0.22 mmol), PyBOP (90 mg, 0.17 mmol), and DIEA (0.55 mmol) in DMF (1 mL) was stirred at rt for 3 h. After removal of DMF under the reduced pressure, the product was extracted with AcOEt and 10% citric acid. The organic layer was washed with Sat. NaHCO₃, brine, and dried (anhyd. Na₂SO₄). The crude material was purified by SiO₂ column chromatography (AcOEt / hexanes = 2/3 to 1/1) to give the product as a colorless amorphous solid, 113 mg, 67%. ¹H NMR (400 MHz, CDCl₃) δ 1.43–1.47 (58H, Boc × 6, γ, δ-CH₂ Lys), 1.69–1.85 (9H, 3,4,5-CHCH₂), 1.96–2.00 (m, 1H, β-CH_a Lys), 2.08–2.12 (m, 1H, β-CH_b Lys), 3.07–3.16 (14H, 3,4,5-CH₂NHBoc, and CH₂NHFmoc Lys), 4.04–4.16 (7H, 3,4,5-OCH₂, FmocCH), 4.85 (m, 1H, α-CH Lys), 5.00 (t, 1H, *J* = 4.8 Hz, NHFmoc), 5.18 (d, 1H, *J* = 12.2 Hz, CH_{2a}Ph), 5.22 (d, 1H, *J* = 12.2 Hz, CH_{2b}Ph), 5.43–5.81 (6H, 3,4,5-NHBoc), 6.96 (d, 1H, *J* = 7.0 Hz, PhCONH), 7.06 (s, 2H, aromatic form gallate), 7.26–7.39 (m, 9H, aromatic from Fmoc and Benzyl), 7.54 (d, 2H, *J* = 7.5 Hz, aromatic from Fmoc), and 7.73 ppm (d, 2H, *J* = 7.6 Hz, aromatic from Fmoc).

4.1.2.6. N-[3,4,5-Tris[3-(1,3-(N,N'-tert-butoxycarbonyl)diaminopropyl]-1-propanoxy]benzoyl-L-lysine (9). Compound 8 (102 mg, 0.067 mmol) was treated with 20% diethylamine in DMF for 1 h. Immediately after concentration, the product was used for the next reaction without further purification.

4.1.2.7. N-[3,4,5-Tris[3-(1,3-(N,N'-tert-butoxycarbonyl)diaminopropyl]-1-propanoxy]benzoyl-N'(BODIPY-PEG₄)-L-lysine benzyl ester (10). A solution of compound 9 (0.067 mmol), BODIPY (30 mg, 0.093 mmol), HOBt (24 mg, 0.16 mmol), PyBOP (54 mg, 0.10 mmol), and DIEA (0.15 mmol) in DMF (3 mL) was stirred for 18 h. After work up the reaction, the crude material was purified by SiO₂ column chromatography (chloroform/MeOH = 50/1) to give the product as a red solid, 106 mg, 99%. ¹H NMR (400 MHz, CDCl₃) δ. 1.43 (58H, Boc × 6, γ, δ-CH₂ Lys), 1.69–1.96 (11H, 3,4,5-CHCH₂, β-CH₂ Lys), 2.37–2.43 (8H, BODIPY-CH₂, CH₃-dipyrrin × 2), 2.49 (s, 6H, CH₃-dipyrrin × 2), 3.05–3.25 (16H, 3,4,5-CH₂NHBoc, BODIPY-CHCH₂ and ε-CH₂ Lys), 4.04 (br, 6H, 3,4,5-OCH₂), 4.81 (m, 1H, α-CH Lys), 5.18 (d, 1H, *J* = 12.2 Hz, CH_{2a}Ph), 5.22 (d, 1H, *J* = 12.2 Hz, CH_{2b}Ph), 5.57 (br s, 6H, 3,4,5-NHBoc), 6.00 (s, 2H, CH-dipyrrin), 6.83 (d, 1H, *J* = 7.5 Hz, PhCONH), 6.98 (s, 2H, aromatic form gallate), and 7.32–7.36 ppm (m, 5H, aromatic from Benzyl): LRMS-ESI (*m/z*): [M+Na]⁺ Calcd for C₈₁H₁₂₅BF₂N₁₀O₁₉, 1613; found 1613.

4.1.2.8. N-[3,4,5-Tris[3-{1,3-(N,N'-tert-butoxycarbonyl)diaminopropyl]-1-propanoxyl]benzoyl-N'(BODIPY-PEG₄)-L-lysine (11).

Compound **10** (99 mg, 0.062 mmol) was deprotected by hydrogenation under atmospheric hydrogen in the presence of Pd(OH)₂ (10 mg) in MeOH (14 mL). The resulting material was purified by SiO₂ column chromatography to afford the free acid as a red amorphous solid, 58 mg, 62%. LRMS-ESI (*m/z*): [M+Na]⁺ calcd for C₇₄H₁₁₉BF₂N₁₀O₁₉, 1523. Found 1523.

4.1.2.9. N-[3,4,5-Tris[3-{1,3-diaminopropyl]-1-propanoxyl]benzoyl-N'(BODIPY-PEG₄)-L-lysine (12).

Compound **11** (14 mg, 0.009 mmol) was treated with 50% TFA in dichloromethane, and the product was purified by preparative HPLC to give the desired product as a red amorphous solid, 10 mg, 68%. LRMS-FAB (*m/z*): [M+H]⁺ Calcd for C₄₄H₇₂BF₂N₁₀O₇, 901; found 901, HRMS-FAB (*m/z*): [M+H]⁺ calcd for C₄₄H₇₂BF₂N₁₀O₇, 901.5647. Found 901.5643.

4.1.2.10. H-β-Ala-Cys-4ABA-Met-OCH₃, (13).

A solution of **5** (0.13 mmol), Fmoc-β-Ala-OH (80 mg, 0.26 mmol), HOBT (44 mg, 0.29 mmol), DIEA (0.26 mmol), and PyBOP (100 mg, 0.19 mmol) in DMF (5 mL) was stirred overnight. After work up the reaction, the crude material was purified by SiO₂ column chromatography (AcOEt/hexane = 4/1) to give Fmoc-β-Ala-attached peptidomimetics, 58 mg, 65%. ¹H NMR (400 MHz, CDCl₃) δ 2.07 (s, 3H, SCH₃), 2.07–2.12 (m, 1H, γ-CH_a Met), 2.20–2.29 (m, 3H, β, γ-CH_b Met), 2.46 (dd, 1H, *J* = 5.0 and 12.5 Hz, β-CH_a Cys), 2.52–2.58 (m, 3H, NHCH₂CH₂ β-Ala, β-CH_{2b} Cys), 3.07 (t, 2H, *J* = 6.7 Hz, CH₂NHPh), 3.39 (2H, NHCH₂CH₂ β-Ala), 3.75 (s, 3H, OCH₃ Met), 4.09–4.17 (m, 2H, NHPh and FmocCHCH₂), 4.29–4.35 (m, 3H, and CHCH₂NHPh, FmocCHCH₂), 4.87 (m, 1H, α-CH Met), 5.50 (t, 1H, *J* = 5.2 Hz, FmocNH), 5.80 (d, 1H *J* = 7.7 Hz, CONH), 6.44 (d, 2H, *J* = 8.5 Hz, aromatic from benzoyl), 6.77 (d, 1H, *J* = 7.4 Hz, CONH Met), and 7.18–7.74 ppm (m, 25H, aromatic from Fmoc, Trt, and benzoyl): LRMS-ESI (*m/z*): [M+Na]⁺ Calcd for C₅₃H₅₄N₄NaO₆S₂, 929; found 929, LRMS-FAB (*m/z*): [M+H]⁺ Calcd for C₅₃H₅₄N₄O₆S₂, 907. Found 907, HRMS-FAB (*m/z*): [M+H]⁺ Calcd for C₅₃H₅₄N₄O₆S₂, 907.3563. Found 907.3845.

The Fmoc group of the compound was removed by treatment with 15% of diethylamine in DMF for 30 min at rt. After concentration, the product was immediately used for the next reaction without further purification.

4.1.2.11. N-[3,4,5-Tris[3-{1,3-diaminopropyl}-1-propanoxyl]benzoyl-N'(BODIPY-PEG₄)-L-lysyl-β-alanyl-L-cysteinyl-L-valyl-L-isoleucyl-L-methionine (1-BODIPY).

Compound 11. (58 mg, 0.039 mmol) was coupled with βAla-Cys(Trt)-Val-Leu-Met-OtBu (0.093 mmol) using HOBT (12 mg, 0.078 mmol), DIEA (0.082 mmol), and PyBOP (33 mg, 0.063 mmol). After work-up the reaction, the resulting crude material was purified by SiO₂ column chromatography (AcOEt/hexane = 4/1) to afford the fully protected compound as an orange solid, 58 mg, 65%. ¹H NMR (400 MHz, CDCl₃) δ 0.79–0.95 (12H, γ, δ-CH₃ Ile, 2γ-CH₃ Val), 1.39–1.46 (69H, Boc, tBu, γ-CH₂ Ile, and γ, δ-CH₂ Lys), 1.68–2.08 (19H, 3,4,5-CH(CH₂)₂, β-CH Ile, β-CH Val, β-CH₂, SCH₃ Met), 2.26–2.48 (20H, CH₃-dipyrin × 4, BODIPY-CH₂, CH₂CONH β-Ala, β-CH₂ Cys, and γ-CH₂ Met), 3.02–3.39 (3,4,5-CH₂NHBoc, CHNHCH₂ β-Ala, ε-CH₂ Lys), 4.08 (6H, 3,4,5-OCH₂), 4.28–4.78 (4H, α-CH Cys, Val, Ile, Met), 5.59 (6H, BocNH), 6.00 (s, 2H, CH-dipyrin), 6.98 (s, 2H, aromatic from gallate), and 7.20–7.41 ppm (15H aromatic from Trt): LRMS-ESI (*m/z*): [M+Na]⁺ Calcd for C₁₁₉H₁₈₀BF₂N₁₅O₂₄S₂, 2340. Found 2340.

This compound (20 mg, 0.0086 mmol) was dissolved in dichloromethane (900 μL), and triethylsilane (100 mL) and trifluoroacetic acid (1 mL) were added at 0 °C. The solution was stirred at rt for 1 h, and concentrated. The desired product was isolated by

preparative HPLC as a red amorphous solid, 3 mg, 20%. LRMS-ESI (*m/z*): [M+H]⁺ Calcd for C₆₆H₁₁₂N₁₅O₁₂S₂, 1370; found 1370.

4.1.2.12. N-(5-[3,4,5-Tris[3-{1,3-diaminopropyl}-1-propanoxyl]benzoyl-N'(BODIPY)-L-lysyl-β-Ala-Cys-4ABA-Met-OCH₃, (3-BODIPY).

A solution of **11** (45 mg, 0.03 mmol), **13** (0.05 mmol), HOBT (44 mg, 0.071 mmol), DIEA (0.076 mmol), and PyBOP (30 mg, 0.058 mmol) in DMF (2.5 mL) was stirred overnight. After work up the reaction, the crude material was purified by SiO₂ column chromatography to give the fully protected product as an orange solid, 51 mg, 78%. ¹H NMR (400 MHz, CDCl₃) δ 1.43 (58H, Boc × 6, and γ, δ-CH₂ Lys), 1.67–1.88 (11H, 3,4,5-CH₂CH, and β-CH₂ Lys), 2.08 (s, 3H, SCH₃), 2.18–2.64 (22H, CH₂STrt, β, γ-CH₂ Met, CH₃-dipyrin × 4, CH₂CH₂CO β-Ala, and BODIPY-CH₂), 3.01–3.26 (20H, 3,4,5-(CH₂)₂NHBoc, ε-CH₂ Lys, CHCH₂NH, CH₂CO β-Ala, and BODIPY-CH₂CH₂), 3.72 (s, 3H, CO₂CH₃), 3.99 (8H, 3,4,5-OCH₂, and CHCH₂NHPh), 4.70–4.81 (2H, α-CH Lys, and α-CH Met), 5.63–5.85 (6H, BocNH × 6), 6.01 (s, 2H, CH-dipyrin × 2), 6.25 (1H CONH), 6.43–6.60 (2H, CONH × 2), 6.49 (2H, d, *J* = 8.4 Hz, aromatic from benzoyl), 6.86–6.96 (4H, CONH × 2, and aromatic from gallate), 7.31–7.39 (15H, Trt), and 7.60 ppm (d, 2H, *J* = 8.4 Hz aromatic from benzoyl): LRMS-ESI (*m/z*): [M+H]⁺ Calcd for C₁₁₂H₁₆₂BF₂N₁₄O₂₂S₂, 2169; found 2169, LRMS-FAB (*m/z*): [M+Na]⁺ calcd for C₁₁₂H₁₆₁BF₂N₁₄NaO₂₂S₂, 2191; found 2191.

This compound was deprotected by treatment with 50% trifluoroacetic acid in dichloromethane in the presence of 5% triethylsilane. The desired product was corrected by preparative HPLC, 2.4 mg, 13%. LRMS-FAB (*m/z*): [M-BF₃+H]⁺ Calcd for C₆₃H₁₀₁N₁₄O₁₀S₂, 1277; found 1277, HRMS-FAB (*m/z*): [M-BF₃+H]⁺ Calcd for C₆₃H₁₀₁N₁₄O₁₀S₂, 1277.7267. Found 1277.7255.

4.2. Biological evaluations**4.2.1. General**

All reagents used in the biological experiments were purchased from commercial suppliers (Sigma-Aldrich, Bio-Rad, Wako Pure Chemical Industries, Nakarai tesque, Cell Signaling Technology, and Santa Cruz Biotechnology). Recombinant mammalian FTase was expressed and purified by the procedure previously reported.¹⁰ SDS-PAGE and Western blotting were carried out with Miniprotein TGX precast gels (Bio-Rad, 7.5 and 12.5%) using a Bio-Rad Mini-Protean III electrophoresis apparatus.

4.2.2. In vitro FTase assay using microplate reader

In a well of 96-well black plate (Thermo) was placed 10 μL of each stock solution of FPP (final concentration = 5 μM), K-Ras4B peptide (0.01 μM), recombinant FTase (100 nM), and compound (6.25–500 μM) separately, avoiding mixing each other. Adding 160 μL of sample buffer to the well mixed all reagents and initiated the FTase reaction. The time course fluorescence change at 520 nm (ex: 340 nm) was monitored at 30 °C using a microplate reader (SpectraMax M5, Molecular Device).

4.2.3. Confocal imaging

A549 human lung carcinoma epithelial cells were cultured at 37 °C in a humid atmosphere containing 5 % CO₂ in air. Cells were grown in RPMI 1640 (Sigma) supplemented with 10% heat-inactivated fetal bovine serum. Cells (1 mL of 1 × 10⁵ cells/mL) were transferred to a glass dish (Iwaki, 35 × 0.12–0.17 mm) and allowed to adhere to the dish by incubating overnight. DMSO stock solution of compound (10 μM, final DMSO concentration was 0.1%) was added to the cells and incubated for 3 h. The cells were washed for four times with PBS and the dish was filled with Opti-MEM (1 mL, Invitrogen). Images were generated using LSM 5 PASCAL, Carl Zeiss laser scanning microscopy.

4.2.4. Whole cell-based assay

Whole cell-based assay was conducted by a similar method previously reported in the literature (Sebti, Oncogene, 1998). T24 cells and A549 cells were obtained from Health Science Research Resources Bank (JCRB0711) and from Professor Y. Honma (Shimane University), respectively. Cells were plated in MEM (T24) or in RPMI 1640 (A549) and 10% bovine serum on day one, respectively, and treated on day 2 and 3 with either DMSO control, FTI-2153 and GGTI-2154 (50, 100, and 250 μ M) or compound (10, 30, and 100 μ M). The cells were then harvested on day 4 and lysed in lysis buffer (20 mM Tris, pH 7.6, 140 nM NaCl, 2 mM NaF, 1% Triton X-100, protease inhibitor cocktail (Roche)). The lysates (5 μ g) were electrophoresed on a 7.5 and 12.5% SDS-PAGE, transferred to PVDF membrane and immunoblotted, respectively, with anti-HDJ-2 (ab3089) or anti-Rap1A (SC-65). Positive antibody reactions were visualized using peroxidase-conjugated goat anti-rabbit IgG and an enhanced chemiluminescence detection system (GE Healthcare Bioscience).

Acknowledgments

This work was supported by a JSPS Grant-in-Aid for Scientific Research (B/22350074), The Takeda Science Foundation, The Naito Memorial Foundation, and the Eisai Research Foundation. Financial support from GCOE, Osaka University (S. M.). J. O. sincerely thanks Professor Andrew Hamilton (Univ. of Oxford) for discussions on peptidomimetic strategies, and Professor Said Sebti, Norbert Berndt, and Michelle A. Blaskovich (Univ. of South Florida) for their support regarding cell-based assays.

Supplementary data

Supplementary data associated with this article can be found, in the online version, at <http://dx.doi.org/10.1016/j.bmc.2012.09.061>.

References and notes

1. Wells, J. A.; MacClendon, C. L. *Nature* **2007**, *450*, 1001.
2. Robinson, J. A.; DeMarco, S.; Gombert, F.; Moehle, K.; Obrecht, D. *Drug Discovery Today* **2008**, *13*, 944.
3. Kodadek, T. *Curr. Opin. Chem. Biol.* **2010**, *14*, 713.
4. (a) Machida, S.; Kato, N.; Harada, K.; Ohkanda, J. *J. Am. Chem. Soc.* **2011**, *133*, 958; (b) Machida, S.; Usuba, K.; Blaskovich, M. A.; Yano, A.; Harada, K.; Sebti, S. M.; Kato, N.; Ohkanda, J. *Chem. Eur. J.* **2008**, *14*, 1392; (c) Yamaguchi, Y.; Kato, N.; Azuma, H.; Nagasaki, T.; Ohkanda, J. *Bioorg. Med. Chem. Lett.* **2012**, *2012*(22), 2354; (d) Ohkanda, J.; Satoh, R.; Kato, N. *Chem. Commun.* **2009**, 6949.
5. (a) James, G. L.; Goldstein, J. L.; Brown, M. S. *J. Biol. Chem.* **1995**, *270*, 6221; (b) Zhang, F. L.; Kirschmeier, P.; Carr, D.; James, L.; Bond, R. W.; Wang, L.; Patton, R.; Windsor, W.; Syto, R.; Zhang, R.; Bishop, W. R. *J. Biol. Chem.* **1997**, *272*, 10232.
6. Downward, J. *Nat. Rev. Cancer* **2003**, *3*, 11.
7. Friday, B. B.; Adjei, A. A. *Biochim. Biophys. Acta* **2005**, *1756*, 127.
8. Vogt, A.; Qian, Y.; Blaskovich, M. A.; Fossum, R. D.; Hamilton, A. D.; Sebti, S. M. *J. Biol. Chem.* **1995**, *270*, 660.
9. For peptidomimetic FTase inhibitors, see: Knowles, D.; Sun, J.; Rosenberg, S.; Sebti, S. M.; Hamilton, A. D. In *Farnesyltransferase Inhibitors in Cancer Therapy*; Sebti, S. M., Hamilton, A. D., Eds.; Humana Press: New Jersey, 2001; pp 49–64.
10. Cheng, Y.; Prusoff, W. H. *Biochem. Pharmacol.* **1973**, *22*, 3099.
11. Sun, J.; Qian, Y.; Hamilton, A. D.; Sebti, S. *Oncogene* **1998**, *16*, 1467.
12. Sun, Z.; Blaskovich, M. A.; Knowles, D.; Qian, Y.; Ohkanda, J.; Bailey, R. D.; Hamilton, A. D.; Sebti, S. M. *Cancer Res.* **1999**, *59*, 4919.
13. Sun, Z.; Ohkanda, J.; Coppola, D.; Yin, H.; Kothare, M.; Busciglio, B.; Hamilton, A. D.; Sebti, S. M. *Cancer Res.* **2003**, *63*, 8922.
14. Qian, Y.; Marugan, J. J.; Fossum, R. D.; Vogt, A.; Sebti, S. M.; Hamilton, A. D. *Bioorg. Med. Chem.* **1999**, *7*, 3011.